Available online at www.sciencedirect.com
SCIENCE DIRECT®
International Journal of Thermal Sciences 43 (2004) 779–790
International Journal of Thermal Sciences
www.elsevier.com/locate/ijts

Numerical study of transient heat and mass transfer and stability in a salt-gradient solar pond

Ridha Ben Mansour [a], Cong Tam Nguyen [a,*], Nicolas Galanis [b]

[a] *Faculty of Engineering, Université de Moncton, Moncton, New Brunswick, Canada E1A 3E9*
[b] *Department of Mechanical Engineering, Faculty of Engineering, Université de Sherbrooke, Sherbrooke, Québec, Canada J1K 2R1*

Received 20 August 2003; received in revised form 11 February 2004; accepted 24 February 2004

Available online 28 May 2004

Abstract

In this work, the problem of the transient heat and mass transfer and stability within a salt-gradient solar pond has been numerically investigated by mean of a 3D-model with all properties variable as function of temperature and salt concentration. The pond has been subject to real external perturbations resulting from the variations of the local weather conditions. The initial conditions correspond to an 'artificially stabilized' pond with the linear temperature and salinity profiles in the gradient zone. Numerical results as obtained for a Tunisian experimental test-site have been satisfactorily compared and validated against measured temperature data. They have clearly shown that after a relatively short period of operation, say only a few days, the changes in the weather conditions have produced important effects not only on the internal temperature field of the pond, but also on its stability as well. In general, one may expect that some instability could develop and growth from within two critical zones: the first one beneath the water free surface and the second one in the region immediate to the bottom surface. The transient behaviours of the pond, in particular its stability, have also been investigated for a very short period of time, say 24 hours of operation. It has been clearly observed that the overnight cooling at the water free surface may rend unstable the immediate region beneath that surface. On the other hand, the solar heating effect during the daytime may have adverse effect on the stability near the bottom surface. Finally, results have also shown that the water transparency has an important effect on the pond stability itself. A pond with good transparency water has been found to be more susceptible to instabilities than a poor transparency one.

Keywords: Heat and mass transfer; Transient behaviour; Salt-gradient solar pond; Stability; Solar energy; Numerical simulation

1. Introduction

Due to its wide and potential applications in thermal and solar energy systems such as in heating and desalination, the salt-gradient solar pond, Fig. 1(a), has received a special attention from the researchers over the past decades. Many experimental solar ponds were constructed, operated and instrumented around the world, see, for example, [1–5]. The temporal behaviours of the thermal field within the pond and the adverse effects due to a strong wind on both the mixing of the surface zone as well as on the erosion of the gradient zone have also been observed for a particular solar pond operated in an arid region [3]. Many analytical and numerical works have been published in the domain as well shedding an important insight into the thermal behaviours and the performance of a solar pond under various conditions. In particular, the effects due to several operating parameters such as the extracted heat load imposed on the pond, the boundaries heat losses, the pond depth as well as the thickness of the gradient zone have been thoroughly investigated [6–11]. Most of these studies were concerned, however, with the problem of one-dimensional heat diffusion with a constant salinity profile prescribed along the pond depth. Only in few recent numerical works, the two-dimensional and three-dimensional character of the solar pond have been considered while studying the same problem of heat diffusion [12,13]. In particular, the thermal effect

* Corresponding author. Fax: (506) 858-4082
E-mail address: nguyenc@umoncton.ca (C.T. Nguyen).

1290-0729/$ – see front matter
doi:10.1016/j.ijthermalsci.2004.02.018

Nomenclature

C_p	specific heat of the fluid	kJ·kg^{-1}·K^{-1}	
C_s	humid heat capacity of air	kJ·kg^{-1}·K^{-1}	
D	coefficient of salt diffusion	m^2·s^{-1}	
k	thermal conductivity of the fluid	W·m^{-1}·K^{-1}	
P_a	partial pressure of water vapor in ambient air	mm·Hg	
P_s	vapor pressure of water at the surface temperature	mm·Hg	
P_t	atmospheric pressure	mm·Hg	
q_0	incident solar radiation upon the free surface of the pond	W·m^{-2}	
Q_c	the convective heat loss	W·m^{-2}	
Q_{ev}	the evaporation heat loss	W·m^{-2}	
Q_r	the radiation heat loss	W·m^{-2}	
S	salinity	(kg of salt)· (kg of solution)$^{-1}$	
S_h	heat source generating from the solar absorption (Eq. (10))	W·m^{-3}	
t	time	s	
T	saline temperature	K	
T_a	ambient temperature	K	
T_g	ground temperature	K	
T_{sky}	sky temperature	K	
X, Y, Z	spatial coordinates along axes	m	
U_g	heat transfer coefficient of the ground	W·m^{-2}·K^{-1}	
V	wind average velocity	m·s^{-1}	

Greek letters

Φ	relative humidity	
α	coefficient of thermal expansion	K^{-1}
β	coefficient of salt expansion	
ε_w	emissivity of the water free surface, fixed to 0.97	
λ	latent heat of evaporation of water	kJ·kg^{-1}
μ	extinction coefficient (Eqs. (9), (10))	m^{-1}
ρ	fluid density	kg·m^{-3}
σ	Stefan–Boltzman constant	W·m^{-2}·K^{-4}

Indices

a	ambient condition
g	ground
r	reference condition (293.15 K)
s	surface

due to the underground was also taken into account [13]. With regard to the pond stability that constitutes, as stated before, a major factor in its operation and performance, it has been studied by several researchers who employed, in most cases, the well-known linear perturbations theory (see in particular [14–19]). Results as obtained from these studies have provided meaningful details and information regarding the onset of the instabilities, the map of marginal stability of the pond as well as the existence of several possible stable or unstable states that may be encountered in the pond depending upon the ratio of the thermal Rayleigh number with respect to the salinity Rayleigh number (see, for example, [14,15,18,19]). The influence of the radiation absorption and that due to the variability of the diffusivities of the saline solution on the pond stability has also been investigated [19]. It should be noted, however, that due to the assumption of infinitesimal perturbations used in the above studies, the results obtained cannot be, in principle, applied to a real situation where the pond is often subject to rather large and drastic perturbations resulting from rapid changes in the weather conditions. In a very recent work, the authors have studied the transient behaviours of a three-dimensional pond considering both the transfer of mass and energy and variable properties of the saline solution [20]. The results have shown, in particular, that the solar radiation absorption as well as the heat losses through the pond free surface may have adverse effects on the long-term stability of the pond. In the present paper, we are interested to investigate the temporal evolution of the pond stability during a short period of time for a test-site under the influence of real external perturbations in Tunisia.

2. Mathematical modelling

2.1. Governing equations

We study the problem of the transient behaviours of the thermal and concentration fields inside a solar pond as well as its stability in time. Fig. 1(b) shows the geometry of the system under consideration, which consists of a parallelepiped basin of saline solution. The physical properties of the latter (thermal conductivity, density, thermal and salt diffusion coefficients) vary as function of both the temperature and the salinity. The solar pond under consideration has a surface area of 100 m^2 and a depth of 2.2 m. It is subject to a solar radiation and heat exchanges through all of its boundaries. We also assume that at the beginning, the pond is 'artificially stabilized' so that the convection currents can be considered negligible and remain as such during the period of operation.

The process of heat and mass transfer within the solar pond is governed by the following general equations of conservation resulting from the principle of conservation of energy and species:

$$\partial(\rho C_p T)/\partial t = \nabla \cdot (k \nabla T) + S_h \tag{1}$$

$$\partial(\rho S)/\partial t = \nabla \cdot (\rho D \nabla S) \tag{2}$$

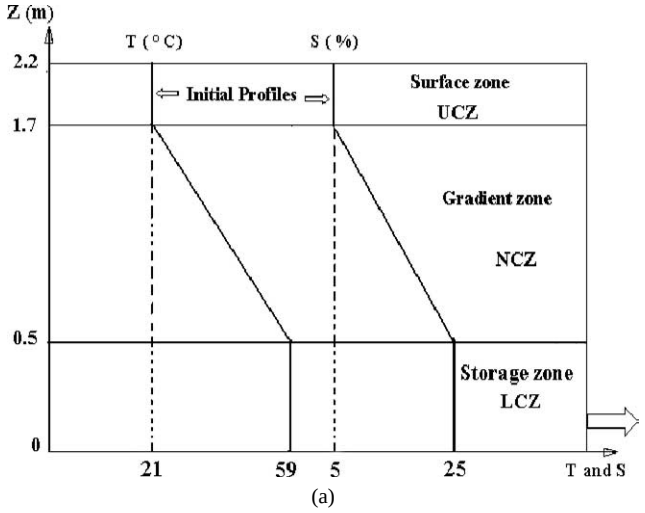

(a)

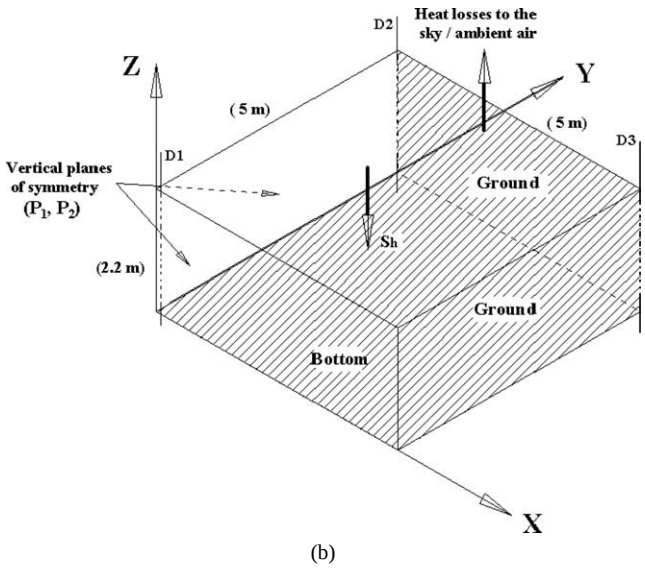

(b)

Fig. 1. (a) Illustration of a salt-gradient solar pond and initial conditions used; (b) Geometry of the solar pond under study.

with the equation of state of the saline solution given as follows [21]:

$$\rho = \rho_r\big[1 - \alpha(T - T_r) + \beta(S - S_r)\big] \tag{3}$$

In the above equations, T and S are, respectively, the saline solution temperature and salinity (i.e., the mass fraction of salt in the solution); α and β are the coefficients of thermal and salt expansion; the subscript 'r' refers to the reference temperature of 20 °C. All of the fluid properties are variable as function of T and S according to known formulas published in the literature. The mathematical expressions of the fluid properties have been summarised in [30]; see also [8,21,22].

The source term S_h in Eq. (1). This term represents the rate of energy generation per unit volume in a layer resulting from the absorption of the solar radiation by the saline solution. In the present study, we assume that the amount of solar radiation (mostly in short wave radiation range) reaching a certain depth Z in the pond suffers an exponential decays as follows [18,24,25]:

$$q_Z = 0.6q_0 \exp\big(-\mu(2.2 - Z)\big) \tag{4}$$

where q_0 is the solar radiation incident on the water free surface, which is assumed to be normal to that surface [18].

The expression for S_h is then as follows:

$$S_h = \partial q_Z/\partial Z = 0.6\mu q_0 \exp\big(-\mu(2.2 - Z)\big) \tag{5}$$

where μ is the extinction coefficient that represents the transparency of the saline solution. In general, the values of this parameter μ are obtained by least-square fitting of Eq. (4) to the experimental values of radiation absorption in pure water and in samples taken from an experimental pond [23]. In the absence of such data, we have chosen in this study some typical values for this coefficient, say $\mu = 0.2$ and 0.8 m^{-1}; the first value corresponds, in fact, to the pure water that exhibits minimum radiation absorption, i.e., good transparency, while the second one corresponds approximately to a weak transparency condition that is often encountered in an experimental solar pond. In general, it is believed that for a low value of μ, the pond will develop greater temperature gradient for the same solar radiation input, and as a result, it would likely be more susceptible to instabilities than a poor transparency one [18]. The complete details regarding the above exponential attenuation model as well as its validation may be found in [24,25].

2.2. Boundary and initial conditions

The appropriate boundary conditions are detailed in Appendix A. As initial conditions, we assume that at the beginning of the operation period, i.e., at the time $t = 0$, the pond has been '*artificially stabilized*' so that in the gradient zone, both the temperature and salinity increase linearly as function of the depth towards the bottom, while in the surface zone and the storage zone, the fluid temperature and its salinity are considered to be uniform. These initial conditions are shown in Fig. 1(a). Note that the same conditions were consistently used when performing parametric studies.

3. Numerical method and validation

The resolution of the system of governing equations (1), (2) subject to the boundary conditions and constitutive equations has been successfully carried out by employing the powerful FLUENT code [28] that is based essentially on the 'finite-control-volume approach' where each of the governing equations is integrated over finite control-volumes. The heat and mass fluxes through the boundaries of any control-volume have been evaluated using the well-known exponential scheme [29]. For the treatment of the transient term in Eqs. (1), (2), we have used a fully implicit second order

scheme among several options offered by the code. Such an implicit scheme ensures, in principle, the stability of the solution regardless the size of the time step used. More details regarding this numerical scheme may be found in [28].

The algebraic 'discretised equations' resulting from the above integration process have been solved sequentially within each time step using the well-known TDMA ('Tri-Diagonal Matrix Algorithm') technique. For all the numerical experiments performed in this work, a time step Δt varying from 1 to 3 hours has been found to be quite appropriate for the task demanded. A converged solution has satisfactorily been achieved with a residue as small as 10^{-5} and 10^{-6}, respectively, for the equation of salinity and energy.

In order to ensure the consistency as well as the accuracy of the numerical results, several non-uniform grids have been submitted to an extensive testing procedure. These results, see [30], have clearly shown that the $50 \times 50 \times 60$ non-uniform grid appears to be largely sufficient to ensure an adequate precision of the numerical results. The adopted grid has respectively 50, 50 and 60 nodes along the directions X, Y and Z with highly packed grid points along all the boundaries of the domain.

The computer program has been extensively and successfully validated by comparing the calculated temperature field with available analytical data for several steady-state cases. The quantitative comparison was also carried out by performing a transient case on the test pond using real weather data [12] from Tunis. The complete details regarding the study of the grid independence, the model validation as well as other numerical information are presented elsewhere, see [30] and also [31].

4. Results and discussion

In order to study the stability of the pond and its time evolution, the following 'stability parameter' has been defined:

$$F_s = (1/\rho_r)(\partial\rho/\partial z) = -\alpha\partial T/\partial z + \beta\partial S/\partial z \tag{6}$$

The solar pond is qualified as stable if $F_s \leqslant 0$ while $F_s = 0$ corresponds to the marginal stability condition. In the following, the results as obtained for the test-pond located in Tunis during the specific period of time from June 20th to June 26th 1993 are presented and discussed with emphasis on the transient thermal behaviors of the pond and its stability in time. The value of the coefficient of extinction μ has been fixed to 0.8 m^{-1}, unless otherwise noted. All weather data such as solar radiation, wind velocity, ambient air temperature and humidity, have been obtained from published information [12].

4.1. The transient behaviours of the pond during one week of operation

Fig. 2(a)–(c) show, respectively, the temporal development of the temperature profile of the saline solution along three specific vertical lines named D_1, D_2 and D_3 (see Fig. 1(b) for their locations). Although a similar pattern has been observed for these profiles, we can easily notice the difference in the values of the temperature from one location to another; this confirms quite eloquently the three-dimensional character of the thermal field. It is also observed that, in general, fluid temperature continuously increases with time and this throughout the pond depth; such behaviour results obviously from the solar energy absorption process. Thus, in the central region along the line D_1 (Fig. 2(a)), one can observe that only a few days after the beginning of operation, the initial temperature profile has been drastically modified. Three different zones may be noticed through the pond depth. The first zone, very thin, says just about few centimetres of thickness, is located near the water free surface and is characterized by the existence of a relatively high temperature gradient along the Z-axis. Such behaviour is essentially due to the important absorption of solar energy by the saline solution in this surface zone. This solar energy absorption also affects greatly the central region of the pond (the gradient zone). In this zone, we can observe that the saline temperature tends to become more homogenous and the temperature gradient steadily and progressively decreases with time. In the third zone (the storage zone), located behind the pond bottom, is characterized by the highest temperature of the saline solution, say about 67 °C. In this zone, one can also observe that the initial uniformity of the fluid temperature does no longer exist.

In the regions along the lines D_2 and D_3, see Fig. 2(b) and (c), one can observe the striking effects due to the heat losses through the lateral walls and the bottom surface of the pond on the temperature profile, in particular in the lower region near the bottom. In the latter, the fluid temperature clearly decreases with increasing time. This is due to the heat losses to the surrounding ground, which is more pronounced near the lateral walls and, in particular, in the lower region where hot fluid is confined; as consequent, the temperature difference between the fluid and the ground (assumed at 7 °C) is more important. Such heat losses towards the ground is indeed much more important in the lower corner region along the line D_3 since they result from the combination of three different surfaces in space. We can also see that at the pond bottom, the fluid temperature has decreased nearly by 11 °C between the centre area (along D_1) and the corner area (along D_3).

With regard to the time-evolution of the salinity field during the same week of operation considered, it has been observed that the salinity profile along the depth axis Z remains essentially unchanged with time. Such behaviour appears physically realistic since it is well known that the mass diffusion of salt is rather slow with respect to that of the heat diffusion (the coefficient of the mass diffusion of salt is about 10^{-9} $m^2 \cdot s^{-1}$). Therefore, for a short period of time as the one under consideration here, there would be, practically, no perceptible changes in the salinity field (see [20]).

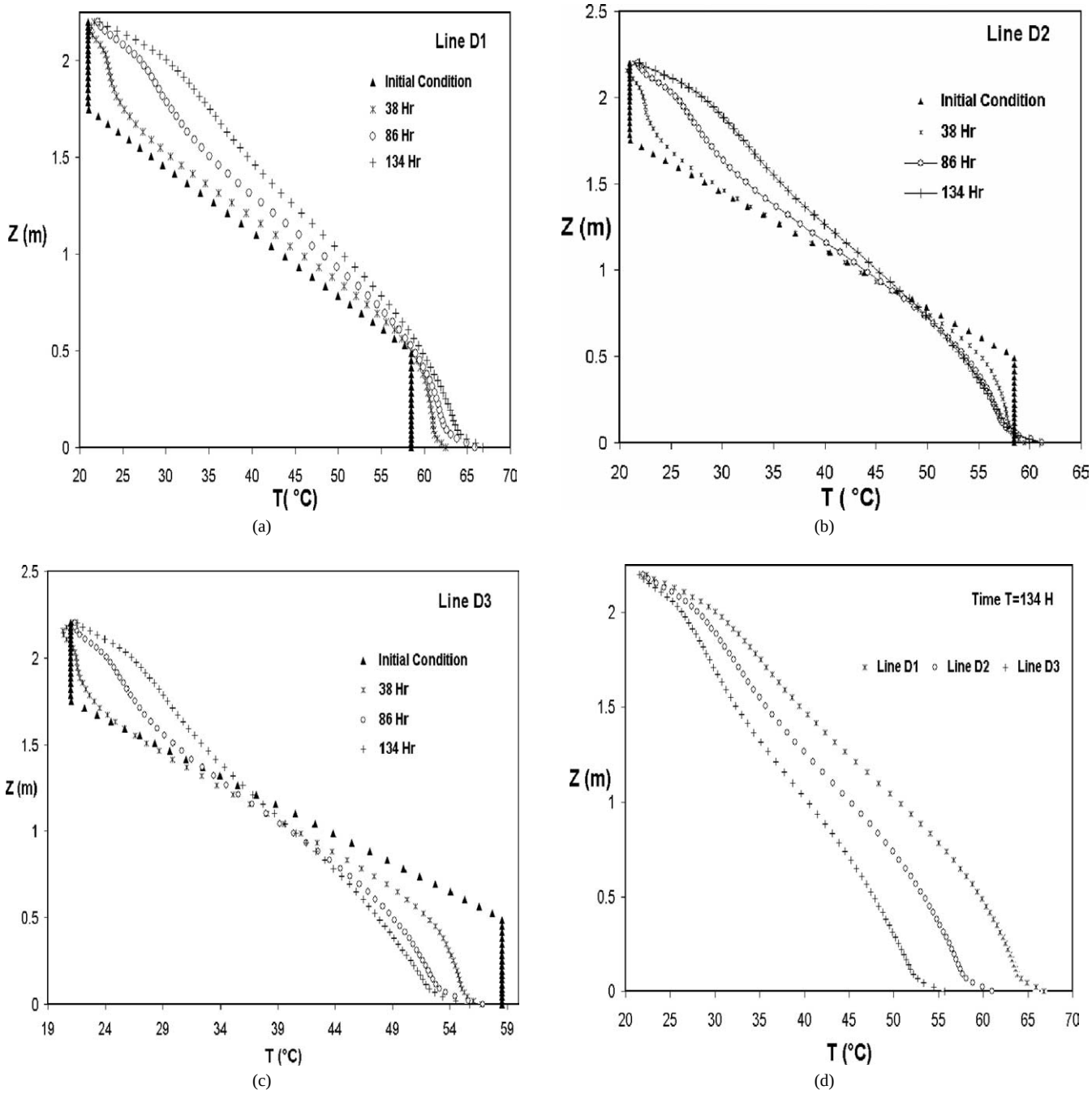

Fig. 2. Temporal development of the temperature profile during a week of operation.

In order to study in details the dynamic behaviours of the solar pond during the same week of its operation, we have established the time-evolution of the stability parameter F_s along the three lines D_1, D_2 and D_3 considered previously, Fig. 3(a)–(c). It is observed, at first, that except for some differences in its values, the profiles shown for F_s exhibit nearly the same pattern from one line to another. Thus, we can see that, in general, there exist clearly two critical zones in the pond where the value of F_s is positive. The first critical zone, of the thickness about 40 cm, is located beneath the water free surface. In this region, the parameter F_s is generally positive and it increases clearly with time. It is also very interesting to observe that in the vicinity of the free surface, say within the depth of about 5 cm, the parameter F_s, which is initially negative (i.e., this tiny region was initially under stable condition), has changed its sign to positive only after few days of operation, and it continues to increase considerably with the augmentation of time. Thus, for example, at the location of the central line D_1 and on the free surface, F_s has increased from – 0.005 m^{-1} at the time $t = 38$ Hr to 0.027 m^{-1} at $t = 134$ Hr. This indicates clearly that under the solar heating effect, some instabilities

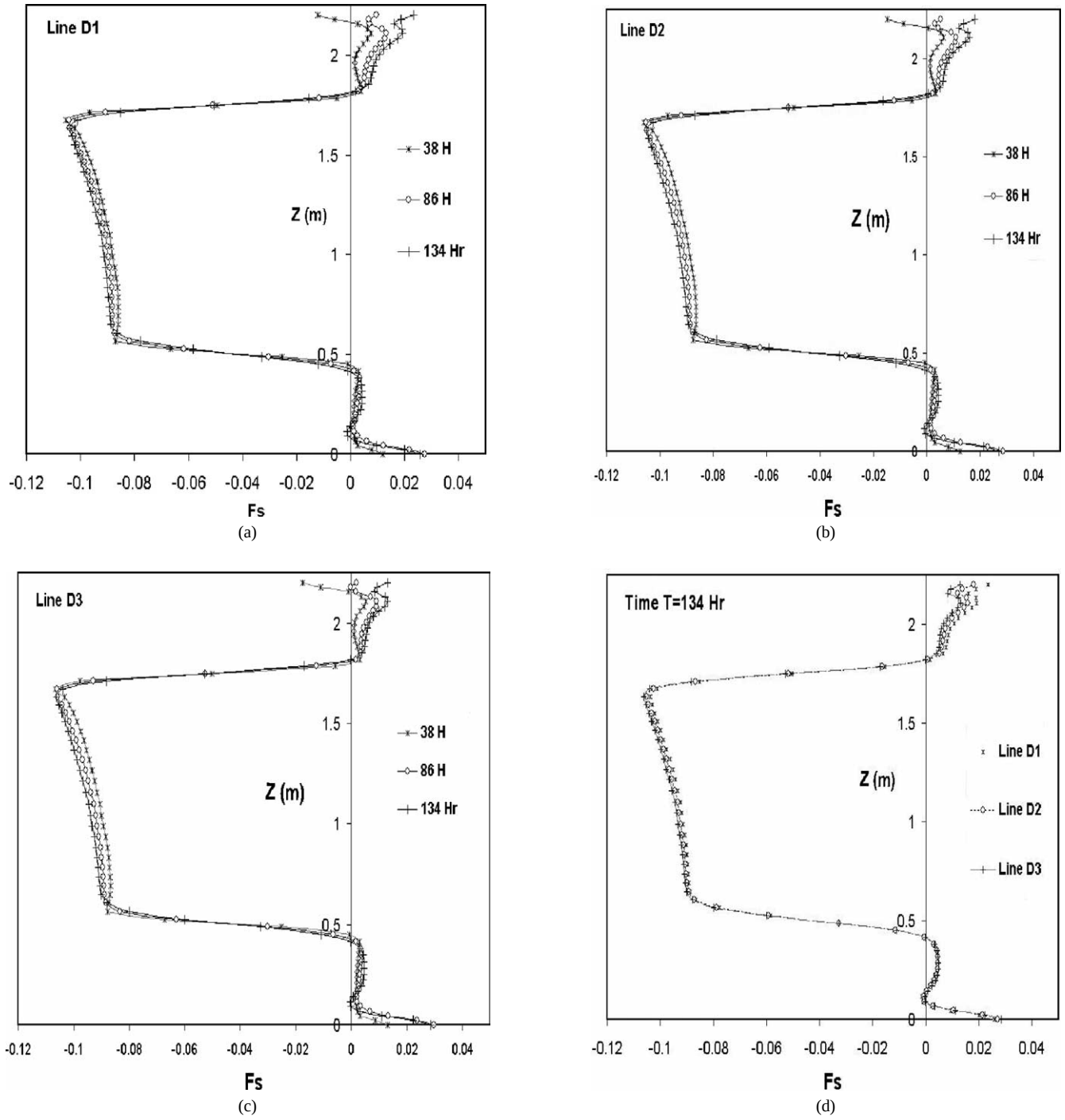

Fig. 3. Temporal development of the stability profile during a week of operation.

may develop in time in the region immediate to the free surface. The second critical zone is observed behind the bottom surface of the pond and has a thickness of about 40 cm that appears to remain constant in time. One can observe that in this zone, over a first portion of about 30 cm, the parameter F_s, although positive, remains relatively low. However, in the second portion of the zone, about 10 cm in depth before reaching the pond bottom, the positive value of F_s increases considerably with the depth and it has reached its maximum $\approx 0.025\ \mathrm{m}^{-1}$ on the bottom surface. Hence, as stated before for the first critical zone, instabilities may develop as well from within the bottom zone as well. It is very interesting to mention here that the above behaviours appear to be consistent with other observations and results, see in particular [22]. Fig. 3(d) shows finally the comparison of the profiles for F_s as obtained along the three lines considered earlier and at a specific time $t = 134$ Hr. The same pattern, again, can be observed here through these

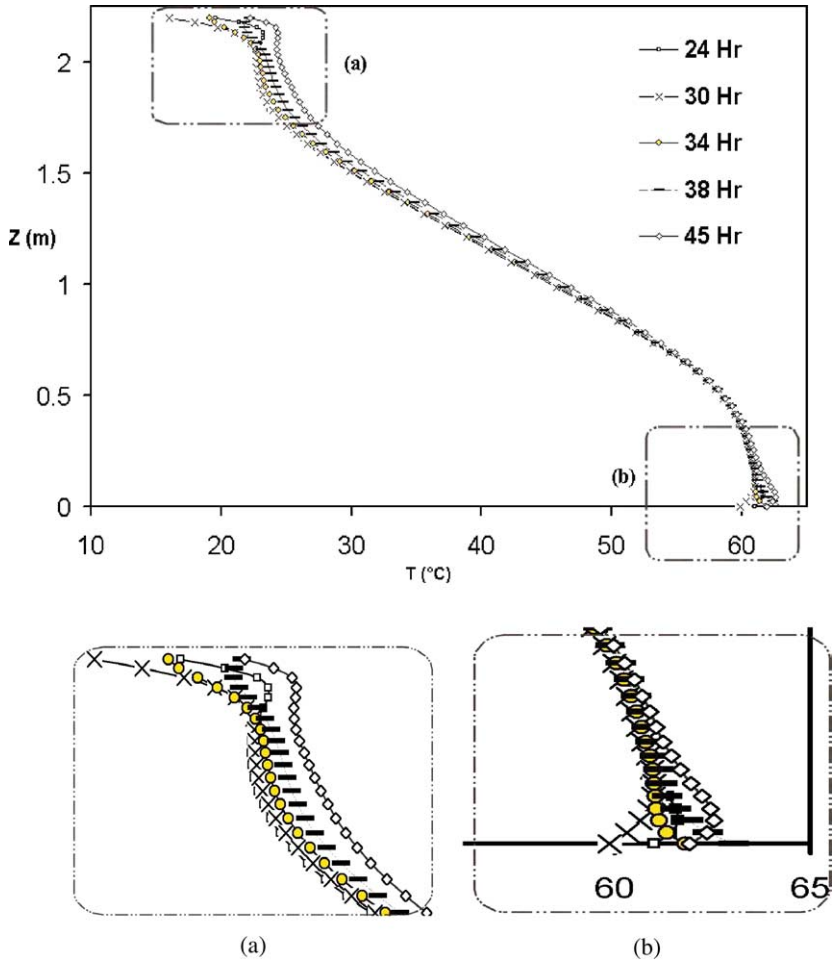

Fig. 4. Temporal development of the temperature profile during a period of 24 hours.

profiles. Also, the boundaries of different critical zones as discussed previously remain identical for the locations shown. In the first critical zone near the free surface however, some notable change in the values of the parameter F_s has been noticed. Thus, it is observed that the positive value of F_s seems to be higher in the central region (near line D_1) indicating that the fluid would become more unstable than elsewhere in the solar pond, for example, while compared to the areas near lines D_2 (near the lateral wall) and D_3 (near the corner). In fact, the surface region around the corner appears to be the least unstable among the three. Such behaviour may be attributed to the heat losses to the underground, which are more pronounced in the regions near the lateral walls. As consequent, the fluid gradient temperature along the Z-axis is lower in these regions, and hence, the fluid would be less unstable than the one confined in the central region.

4.2. The transient behaviours of the pond during a 24 hours of operation

In view of the transient behaviours of the pond for a week of operation as discussed previously and because of the rapid and drastic changes in the weather conditions such as wind velocity, air temperature and humidity and solar radiation incident upon the pond free surface, we have attempted to study the temporal evolution of the temperature and salinity fields as well as the pond stability for a very short period of time, say for the period of 24 hours starting from midnight June 20th to midnight June 21st 1993.

Fig. 4 shows, at first, the temporal evolution of the temperature profile along the line D_1 during the period considered. For discussion purpose, Fig. 5(a) also shows the time variation of different temperatures as well as that of the incident solar radiation q_0 upon the pond free surface; and Fig. 5(b) shows the temporal evolution of the heat losses or gains through the two surfaces of interest, the water free surface and the pond bottom surface. One can observe, Fig. 4, that there are clear changes in the temperature profile with time, in particular within the two critical zones discussed previously (the first zone beneath the free surface and the second one behind the pond bottom). Thus, in the first zone, it has been observed that initially, i.e., at $t =$ 24 Hr or midnight of June 20th, the fluid temperature has slightly decreased towards the water surface. Such behaviour may be attributed to the important heat losses from the

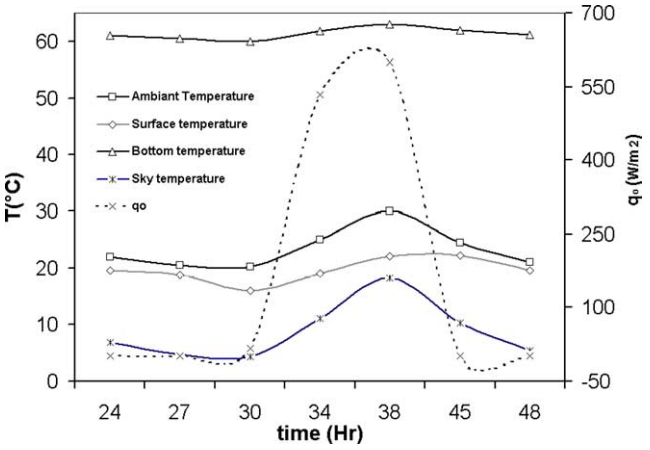

(a)

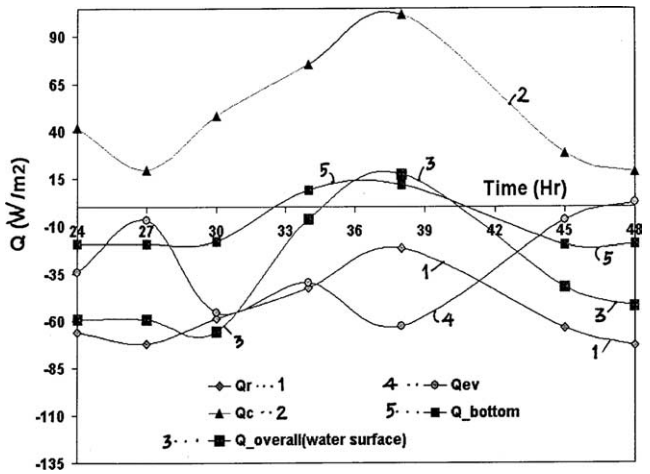

(b)

Fig. 5. (a) Time variation of temperatures and solar radiation during a period of 24 hours; (b) Time variation of heat losses and gains through the water surface and the bottom.

free surface towards the surrounding environment during the night, especially the heat loss by radiation to the sky that has been found to be the most dominant at that time, say nearly 66% of the total heat loss through the water surface, see Fig. 5(b). With the increase in time, say after six hours of operation, i.e., at the time $t = 30$ Hr or 6 o'clock in the morning of June 21st, the heat losses are becoming even more important and as consequent, the water temperature at the free surface has, in fact, dropped from 19.6 °C at the time $t = 24$ Hr to 16.5 °C at the instant $t = 30$ Hr, Fig. 5(a). During that interval of time, the overall heat loss from the free surface is approximately the maximum for the 24 hours period, Fig. 5(b). During the daytime, say the period of time between $t = 34$ Hr and $t = 38$ Hr, the solar radiation incident upon the pond surface becomes much more important, $H_s \geqslant 533$ W·m^{-2}, see Fig. 5(a), which has induced an important heating effect on the water surface during that period of time. Such favourable effect, combined to some small heat gain from the ambient air has induced a strong heating on the upper layer of the pond. Thus, as we can notice, the water temperature at its free surface has considerably increased in time to reaching nearly 22 °C at the instant $t = 38$ Hr or 2 o'clock in the afternoon of June 21st 1993. The surface temperature remained nearly constant afterwards; in the evening, it started to decrease again under the effects of heat losses. With regard to the storage zone located behind the bottom surface, it is observed that during the daytime, under the effects of solar energy absorption (Fig. 5(b)), the temporal gradient of the fluid temperature is positive and the bottom surface temperature has reached its maximum of about 64 °C at the time $t = 38$ Hr. During the night time however, with no solar energy input, the fluid temperature also decreases with time, which is, as stated before, due obviously to the heat losses towards the underground. We can also observe that the temporal variation of the bottom surface temperature appears to be considerably less pronounced than that of the free surface temperature. Such behaviour can be explained by the fact that the bottom zone is, practically, not much affected by the changes in the weather conditions and the thermal boundary conditions at the walls and the bottom surface are remaining constant with time. Furthermore, the absorption of solar energy by the bottom surface during the daytime is remained relatively weak, as the coefficient of extinction μ has been fixed to 0.8 m^{-1}.

Fig. 6 shows finally the time evolution of the stability parameter F_s for the period considered. We can observe that within the two critical zones mentioned previously, there is a remarkable change in the F_s profile with time. Thus, during the night time and in the upper zone of the pond, the parameter F_s remains positive and has reached its maximum of about 0.038 m^{-1} on the water free surface at the instant $t = 30$ Hr. Such behaviour, as discussed above, is a direct consequent of the overnight cooling of the water in the vicinity of the pond free surface. Hence, one can expect some forms of instabilities that may be generated from within this surface region. It is interesting to note that strong values of F_s are observed within the depth of about 20 cm beneath the free surface. In contrast, in the storage zone and in the absence of solar radiation absorption during the nighttime, the heat losses towards the underground have positive effects on the local stability. Between the two instants $t = 30$ Hr and $t = 38$ Hr, i.e., between 6 o'clock of the morning and 2 o'clock in the afternoon of June 21st 1993, one can notice a striking change on the profile of F_s in the upper zone. Thus, F_s, although remaining positive at the free surface, has decreased clearly from $t = 30$ Hr to the time $t = 34$ Hr. At the instant $t = 38$ Hr in particular, F_s even turns to negative at the free surface. That is, under the solar heating effect, the surface water has been heated up (see again Fig. 5(a)) and as result, and it has become more stable. Note that the newly formed stability zone is really located on the water free surface, say within few centimetres beneath the latter; while the adjacent part of the upper zone is still under the risk of instabilities, i.e., $F_s > 0$. During the

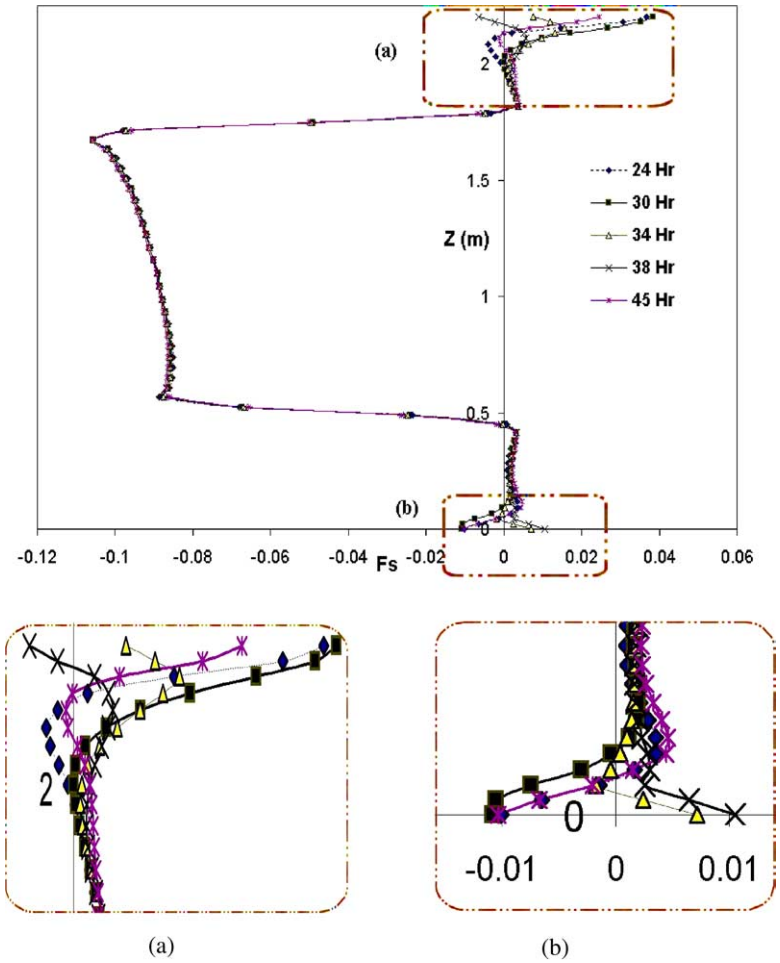

Fig. 6. Time variation of the stability characteristics during a period of 24 hours.

evening, say at $t = 45$ Hr or 9 o'clock, under the effect of cooling discussed previously, the parameter F_s at the free surface has turned again to positive, and the cycle continues. On the other hand, in the lower zone near the pond bottom and during the daytime, say for time between 30 and 38 Hr, the fluid temperature at the bottom surface has increased (see again Fig. 5(a)). This has rend unstable the region behind that surface as F_s now becomes positive. For time further than 38 Hr, F_s has decreased and become negative again, at the time $t = 45$ Hr for example, which coincides with the cooling of the bottom zone (see Fig. 5(b)). We can see that the variation of F_s appears considerably less pronounced than that in the surface zone, for the same reasons mentioned previously. In summary, the numerical results presented here have clearly shown that the heat losses from the solar pond to the atmosphere as well as the solar heating effect on the bottom surface may have adverse effects on the pond stability, and this even for a very short period of time. These results, which are believed to be the first of the kind, have in fact provided very interesting details regarding the dynamic behaviours and the stability of a salt-gradient solar pond.

4.3. The effects of the water transparency on the pond stability

The water transparency, which is characterized by the so-called the coefficient of extinction μ of the water (see Eqs. (4) and (5)) is expected to play an important role not only on the internal temperature field of the pond but also on its stability as well, since such transparency has a direct impact on the absorption of the solar energy by the saline solution. In order to study its effects, we have performed calculations for the Tunisian test site considered previously during the same period of time, i.e., from June 20th to June 26th 1993, and this using the same corresponding weather data employed before. The only parameter that has been modified is, of course, the parameter μ, which has taken as value 0.2 m^{-1}(corresponding to a clear water condition). We shall refer, hereafter, to cases 1 and 2 that correspond, respectively, to $\mu = 0.8$ m^{-1} and $\mu = 0.2$ m^{-1}.

The effect due to the change of the parameter μ on the temperature field may be better understood by scrutinizing Fig. 7(a) that shows the temperature profile along the main vertical axis (i.e., line D_1, see again Fig. 1(b)) as obtained for

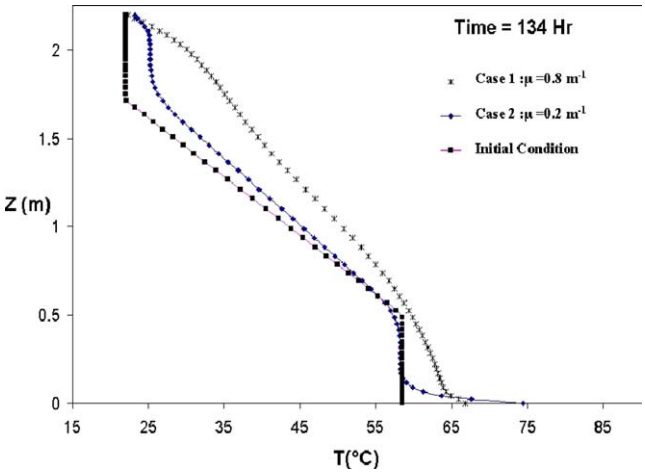

(a)

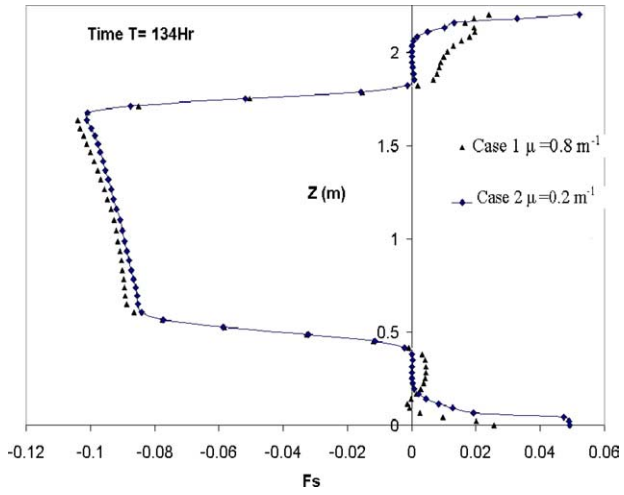

(b)

Fig. 7. (a) Effect of the water transparency on the temperature profile at $t = 134$ Hr; (b) Effect of the water transparency on the F_s-profile at $t = 134$ Hr.

the cases considered at the instant $t = 134$ Hr. We can notice the striking differences between the profiles shown. Thus, as stated before (see again Section 4.1) and with respect to the initial condition, it is observed that the temperature profile has been considerably modified in case 1 where the important solar heating effect appears to be present in a large region, especially in the upper part of the pond. One can also see that the departure from the initial temperature profile appears to be very important where the zones of uniform fluid temperature, which existed at the beginning, do no longer exist in the pond. Such departure appears clearly less pronounced for case 2 where the corresponding temperature profile is closer to the initial one, in particular in the lower central part of the pond. For this case, the solar heating effect does also exist in the vicinity of the bottom surface where the temperature gradient along the Z-axis is, surprisingly, considerably more pronounced than that corresponding to case 1; also, the maximum fluid temperature, nearly 74 °C, occurring on the bottom surface, has been found to be well higher than the value of 67 °C as obtained for case 1. These results may appear somewhat paradoxically but they can be explained by the fact that for case 2, as the attenuation of the traversing solar radiation is less pronounced, the remaining radiation incident on the bottom surface—which is assumed to be a blackened surface—would be more important than the corresponding one of case 1. In fact, the solar radiation upon the bottom surface has been estimated to be $\approx 39\%$ and $\approx 10\%$ of the value of q_0, respectively, for cases 2 and 1. The solar heating effect has also been observed in the upper part of the pond, although it appears clearly less pronounced than in case 1 as mentioned earlier. Thus, for case 2, the maximum temperature difference is only about 5 °C with respect to the initial condition. From the above results, it is clear that for a lower value of μ, i.e., a good transparency pond, the solar heating effect is less important than that of a poor transparency one. Such behavior, which appears physically quite realistic, would have considerable effect on the stability of the pond as well.

Fig. 7(b) shows, finally, the profiles of the stability parameter F_s along the line D_1 as obtained for the cases considered. One can observe, at first, that the two critical zones, one beneath the water free surface and the other one located behind the pond bottom surface, do exist for both cases studied. However, the local values of F_s and the shape of the F_s-profiles within these zones as well as their thickness have drastically changed from one case to another. Thus, it is very interesting to observe that the maximum values of F_s, occurring at both the free surface and the bottom surface, are clearly higher for case 2 than for case 1; for example,fx on the bottom surface, the local maximum is approximately 0.05 and 0.025 m^{-1}, respectively, for cases 2 and 1, the ratio is almost twice between these values. Also, as the parameter μ has changed from 0.8 to 0.2 m^{-1}, the thickness of both critical zones has considerably decreased, by a factor of 2 or even higher. Such results may be explained by the behavior of a good transparency pond regarding its solar heating effect as discussed in details earlier. From the above results of the values of F_s, it is clear that a good transparency solar pond would be more susceptible to instabilities than a poor transparency one. Although a direct comparison with other experimental observations and data was not possible because of a clear lack of such data, it has been found that the above behavior regarding the influence due to the water transparency appears to be consistent with other works in the literature on the solar pond stability (see, for example, [18]).

5. Conclusion

In this paper, we have investigated, by direct numerical simulation, the problem of the transient heat and mass transfer within a salt-gradient solar pond, with emphasis on the influence of the external factors on the its stability characteristics. From the results as obtained for a test pond

in Tunis using the corresponding weather data, the following conclusions seem to be pertinent:

- The solar radiation has an important effect on the internal temperature field and also on the pond stability characteristics. The solar heating effect has been found considerably more important in a poor transparency pond than a good one. For the former, such effect is observed throughout the pond. For the latter, only the surface and bottom regions seem to be affected; the temperature gradient along the depth axis also appears more pronounced, in particular in the vicinity of the pond bottom surface.
- It has been found that there exist two critical zones, one located beneath the water free surface and the other one observed near the bottom surface. It can be expected that some instabilities may take place from within these vulnerable areas, and this even after a short period of time, say several days of operation.
- Regarding the time evolution of the pond characteristics, results have clearly shown that the above critical zones appear to become more vulnerable to instabilities with the increase of time of operation.
- It has been observed that within the critical zones, the solar heating effect as well as the heat losses from the free surface have an important influence on the pond stability characteristics in time, even during a very short period time, say several hours of operation.
- In general, it has been observed that the regions near the lateral walls appear to be less susceptible to instabilities than the interior central areas of the pond.
- Although, the solar heating effect is clearly less important in a good transparency pond, the results have shown that it appears likely to be more susceptible to develop instabilities than a poor transparency one, because of the fact that for the former, the temperature gradient along the depth axis has been found to be more pronounced in the critical zones.

Acknowledgements

The authors wish to sincerely thank the *Natural Sciences and Engineering Research Council of Canada*, the Faculty of Engineering of the '*Université de Sherbrooke*' and the Faculty of the Graduate Studies and Research of the "*Université de Moncton*" for financial support to this project. Thanks are also due to Dr. Jamel Orfi of the Faculty of Sciences of Monastir (Tunisia) for valuable suggestions and to Mr. S.E.B. Maïga for his help in preparing some figures in the final version.

Appendix A. Boundary conditions

The highly non-linear and coupled governing equations (1), (2) must be appropriately solved subject to the following boundary and initial conditions:

- through the lateral walls of the pond, the heat loss to the surrounding ground has been taken into account and is evaluated as follows:

$$Q_{gl} = U_g(T_s - T_g) \tag{A.1}$$

  where the temperature of the ground T_g and the ground heat loss coefficient U_g are estimated to be $T_g = 7\,^{\circ}\mathrm{C}$ and $U_g = 0.36\ \mathrm{W\cdot m^{2}\cdot{}^{\circ}C^{-1}}$, which represent realistically the local conditions at Tunis [12].
- through the pond bottom, we assume that all solar radiation reaching that surface is entirely absorbed, which appears quite realistic since in most cases, the bottom surface is blackened in order to maximize the solar heat absorption. The bottom surface also losses heat into the underground by conduction. The resulting heat exchanges for that surface are as follows:

$$Q_{gr} = -U_g(T_s - T_g) + 0.6q_0\exp(-2.2\mu) \tag{A.2}$$

- through the two vertical planes of symmetry of the pond (see Fig. 1(b)), the usual conditions of zero heat flux and zero mass flux prevail:

$$\begin{aligned} &* \text{ along the plane } P_1\text{:} \quad \frac{\partial T}{\partial X} = \frac{\partial S}{\partial X} = 0 \\ &* \text{ along the plane } P_2\text{:} \quad \frac{\partial T}{\partial Y} = \frac{\partial S}{\partial Y} = 0 \end{aligned} \tag{A.3}$$

  It is important to note here that regarding the boundary conditions for the salinity, a similar zero-mass-flux condition has also been specified along the normal across all the boundaries of the domain.
- at the water free surface, the heat losses by convection and evaporation into the ambient air combined to that between this surface and the sky have been considered. They are summarized as follows:

A.1. The radiation heat loss to the sky is given by

$$Q_r = \varepsilon_w\sigma\left(T_s^4 - T_{\mathrm{sky}}^4\right) \tag{A.4}$$

the sky tempearture T_{sky} is estimated as follows [26]:

$$T_{\mathrm{sky}} = T_a\left[0.55 + 0.61P_a^{0.5}\right]^{0.25} \tag{A.5}$$

with

$$P_a = \Phi\exp\left(18.403 - \left(\frac{3885}{T_a - 43.15}\right)\right) \tag{A.6}$$

A.2. The convective heat loss is given by

$$Q_c = h_c(T_s - T_a) \tag{A.7}$$

with h_c, the wind convective heat transfer coefficient, which depends on the average velocity V of the wind, is given as follows [27]:

$$h_c = 5.7 + 3.8V \tag{A.8}$$

A.3. The heat loss due to evaporation is proportional to the wind convective coefficient h_c and to the difference between the vapor pressure of the water at the free surface and the partial pressure of the water vapor in the atmosphere. The heat loss can be expressed as follows [27]:

$$Q_{\text{ev}} = \frac{\lambda h_C}{1.6 C_s P_t}(P_s - P_a) \tag{A.9}$$

where P_s is the vapor pressure evaluated at the surface temperature:

$$P_s = \exp\left(18.403 - \frac{3885}{T_s - 43.15}\right) \tag{A.10}$$

References

[1] S. Folchitto, Experience with a solar pond at margherita di savoia, in: Proc. 1997 Int. Solar Energy Conf., ASME Publications Solar Engineering, 1997, pp. 223–228.

[2] F.B. Alagao, et al., The design, construction, and initial operation of a closed-cycle, salt-gradient solar pond, Solar Energy 53 (4) (1994) 343–351.

[3] A.M.R. Al-Marafie, et al., Performance of 1700 m^2 solar pond operation in arid zone, Internat. J. Energy Res. 15 (1991) 535–548.

[4] R.L. Reid, et al., Design, construction, and initial operation of a 3355 m^2 solar pond in El Paso, Trans. ASME J. Solar Energy Eng. 111 (1989) 330–337.

[5] A. Joyce, et al., The Portuguese experience on salt gradient solar ponds, in: Proc. Workshop on Solar Ponds, Tunis, Tunisia, December 20, 2001, 5 p.

[6] K. Al-Jamal, S. Khashan, Effect of energy extraction on solar pond performance, Energy Conversion 39 (7) (1998) 559–566.

[7] V. Joshi, et al., A numerical study of the effects of solar attenuation modelling on the performance of solar ponds, Solar Energy 35 (4) (1985) 377–380.

[8] F. Zangrando, On the hydrodynamics of salt-gradient solar pond, Solar Energy 46 (6) (1991) 323–341.

[9] S.G. Schladow, The upper mixed zone of the salt gradient solar pond: Its dynamics, prediction and control, Solar Energy 33 (5) (1984) 417–426.

[10] M.J. Safi, Numerical simulation of a solar pond behaviour, in: Proc. Mediterranean Conference On Renewable Energy Sources For Water Production, Santorini, Greece, 1996, pp. 173–176.

[11] M. Ouini, A. Guizani, A. Belguith, Simulation of the transient behaviour of a salt gradient solar pond in Tunisia, Renewable Energy 14 (1–4) (1998) 69–76.

[12] W. Alimi, Simulation Numérique 3D du stockage du rayonnement solaire dans un étang solaire, D.E.A. Thesis, l'ÉNIT, Tunis, Tunisie, 2001.

[13] M.M. El-Refaee, et al., Transient performance of a two-dimensional salt gradient solar pond—A numerical study, Internat. J. Energy Res. 20 (1996) 713–731.

[14] G. Veronis, Effect of a stability gradient of solute on thermal convection, J. Fluid Mech. 34 (1968) 315–336.

[15] G. Veronis, On finite amplitude instability in thermohaline convection, J. Marine Res. 23 (1) (1964) 1–17.

[16] L.N. Da Costa, E. Knobloch, N.O. Weiss, Oscillations in double-diffusive convection, J. Fluid Mech. 109 (1981) 25–43.

[17] R.S. Schechter, M.G. Velarde, J.K. Platten, The Two-Component Bénard Problem, in: Adv. Chem. Phys., vol. 26, Wiley, New York, 1981.

[18] M. Giestas, H. Pina, A. Joyce, The influence of radiation absorption on solar pond stability, Internat. J. Heat Mass Transfer 39 (18) (1996) 3873–3885.

[19] M. Giestas, A. Joyce, H. Pina, The influence of non-constant diffusivities on solar pond stability, Internat. J. Heat Mass Transfer 40 (18) (1997) 4379–4391.

[20] R. Ben Mansour, C.T. Nguyen, N. Galanis, Transient heat and mass transfer of a salt-gradient solar pond, in: Proc. Eurotherm 71 on Visualization, Imaging and Data Analysis In Convective Heat and Mass Transfer, LTM – UTAP, Reims, France, October 28–30, 2002.

[21] M.A. Darwich, Solar ponds: A seasonal solar energy storage system for process heat application, in: Proc. 1st Saudi Engineering Conference, Jedda, 1983, pp. 1–8.

[22] S.G. Schladow, The dynamics of a salt gradient solar pond, Ph.D. Thesis, University of Western Australia, Australia, 1985.

[23] A.A. Green, A.L.M. Joyce, M. Collares-Pereira, A spectrophotometric method for studying the transmission of radiation in a solar pond, in: Proc. CEC Workshop on Optical Property Measurement Techniques, Joint Research Centre ISPRA, Italy, 27–29 October, 1987.

[24] D.R.F. Harleman, Hydrothermal analysis of lakes and reservoirs, J. Hydraulics Division ASCE Publ. 108 (3) (1982) 302–325.

[25] M. Hondzo, H.G. Stefan, Lake water temperature simulation model, J. Hydraulic Eng. ASCE Publ. 119 (11) (1993) 1251–1273.

[26] G.V. Parmelee, W.W. Anbele, Radiant energy emissions of atmosphere and graund, ASHVE Trans. (1952) 58–85.

[27] V.V.N. Kishore, V. Joshi, A practical collector efficiency equation for non convecting solar ponds, Solar Energy 33 (5) (1984) 391–395.

[28] Fluent 6, User's Guide, Fluent Inc, NH, USA, 2001.

[29] S.V. Patankar, Numerical Heat Transfer and Fluid Flow, Hemisphere, McGraw-Hill, New York, 1980.

[30] R. Ben Mansour, Étude numérique du comportement transitoire d'un étang solaire à gradient de salinité [A Numerical Study of the Transient Behaviors of a salt-gradient solar pond], M.Sc. Thesis, Faculty of Engineering, Université de Moncton, Moncton, NB, Canada, 2003, 148 p.

[31] R. Ben Mansour, C.T. Nguyen, N. Galanis, Transient heat and mass transfer within a salt-gradient solar pond under real external conditions, in: Proc. Int. Symp. TRCON–03, Cesme, Turkey, August 2003, Paper No. TR 10 CT, in press.